

1 This is the peer reviewed version of the following article

2  
3 **Altieri V., De Franco S., Lombardi F., Marziliano P.A., Menguzzato G., Porto P., 2018.**  
4 **The role of silvicultural systems and forest types in preventing soil erosion processes in**  
5 **mountain forests. A methodological approach using Caesium-137 measurements,**  
6 **Journal of Soils and Sediments, Volume 18, Pages 3378–3387, ISSN: 1614-7480**

7  
8 which has been published in final doi <https://doi.org/10.1007/s11368-018-1957-8>

9 (<https://link.springer.com/article/10.1007/s11368-018-1957-8>)

10  
11 The terms and conditions for the reuse of this version of the manuscript are specified in the  
12 publishing policy. For all terms of use and more information see the publisher's website

13

14

15

16

17

18

19

20

21

22

23

24 **The role of silvicultural systems and forest types in preventing soil erosion processes in mountain forests. A**  
25 **methodological approach using Caesium-137 measurements**

26

27 **Valeria Altieri<sup>1</sup> • Silvio De Franco<sup>1</sup> • Fabio Lombardi<sup>1</sup> • Pasquale Antonio Marziliano<sup>1</sup> • Giuliano**  
28 **Menguzzato<sup>1</sup> • Paolo Porto<sup>1</sup>**

29

30 <sup>1</sup>Department of Agraria, University Mediterranea of Reggio Calabria, Feo di Vito, 89123 Reggio Calabria, Italy

31

32 ✉ Paolo Porto

33 paolo.porto@unirc.it

34

35 **Abstract**

36 *Purpose* - Forests play a key role in providing protection against soil erosion. Particularly, the role of vertical forest  
37 structure in increasing rainfall interception capacity is crucial for mitigating raindrop impact and reducing splash  
38 and rill erosion. For this reason, studies on the relationships between forest structures, past management, and the  
39 observed rates of soil loss are needed. In the last decades, importance was given to the use of  $^{137}\text{Cs}$  as radioactive  
40 tracer to estimate soil erosion rates. The  $^{137}\text{Cs}$  technique is linked to the global fallout of bomb-derived  
41 radiocaesium which occurred during a period extending from the mid-1950s to the late 1970s.

42 *Materials and methods* -  $^{137}\text{Cs}$  technique, providing long-term retrospective estimates, could be related to forest  
43 treatments applied during the last decades in different sites, also considering the tree species composition. This  
44 approach could be useful to compare the effect of different canopy cover and biomass on soil erosion rates related  
45 to different tree species. In the work proposed here, a study area dominated by pine and beech high forests located  
46 in the Aspromonte mountain (Calabria, Italy) was selected. The measurements, related to forest structural traits,  
47 focusing on canopy cover and biomass, and also on management approaches and forest types, are compared with  
48 rates of soil erosion provided by  $^{137}\text{Cs}$ .

49 *Results and discussion* - The overall results suggest that minimum values of soil loss are documented in areas with  
50 higher canopy cover and biomass evidencing the protective effect provided by forests against soil erosion. Also,  
51 techniques based on the use of tracers like  $^{137}\text{Cs}$  proved to be helpful to select the best forest management options  
52 useful to optimize the protective role of forests, with the aim to reduce erosion processes in a long-term perspective.

53 *Conclusions* – However, the experiment indicates that care must be taken when new silviculture treatments are  
54 planned. These findings are in agreement with what documented by other authors in similar environments but need  
55 further studies to confirm the effectiveness of using  $^{137}\text{Cs}$  in different forest ecosystems.

56

57 **Keywords** Apennine forests • Beech forests • Caesium-137 • Calabrian pine forests • Silviculture applied • Soil  
58 erosion rates

59

## 60 **1 Introduction**

61 Forests play a key role in providing protection against runoff and soil erosion (Miura et al. 2003). Soil erosion is  
62 a relevant phenomenon in pedogenesis process and affects the evolution of natural ecosystems. Ecological factors  
63 like canopy cover, tree species, forest vertical stratification, but also different types of forest management are  
64 crucial in increasing rainfall interception and reducing the magnitude of soil loss (Elliot et al. 1999; Hartanto et al.  
65 2003). In the last decades, several studies carried out in forest environments stressed the importance of  
66 hydrological functions (Bosch and Hewlett 1982; Moore and Wondzell 2005) and their relationships with soil  
67 degradation (Pennock and Van Kessel 1997). The most serious risk, however, is related to soil erosion by water,  
68 which is one of the most pressing environmental threats worldwide (Reich et al. 2000). Examples in Mediterranean  
69 areas are reported, among the others, by Conacher and Sala (1998) and Montanarella (2007).

70 The effort to mitigate soil erosion is a prerequisite to provide the self-preservation of forest areas, in order to  
71 perform a sustainable forest management. This topic was widely studied in Italy by several researchers (Zanchi  
72 1988; Ollesch and Vacca 2002; Bagarello et al. 2010) and experiments dealing with soil erosion measurements are  
73 also available (Alcamo et al. 2007; Sanchis et al. 2008). However, despite the utility of studies carried out in  
74 experimental plots and catchments to quantify runoff and soil loss, some difficulties to extrapolate the results in  
75 larger areas where no direct measurements are available have emerged. These difficulties are mainly related to the  
76 scale effect in the attempts to extrapolate across the landscape modelled rates of water erosion based on plots (see  
77 Evans and Boardman 2016; Evans et al., 2016).

78 The need to test alternative approaches to collect more information on larger areas suggested the use of Caesium-  
79 137 ( $^{137}\text{Cs}$ ) to provide reliable estimates of soil erosion both at plot (Porto and Walling 2012a,b) and at catchment  
80 scale (Porto et al. 2001; 2009).  $^{137}\text{Cs}$  is a manmade radionuclide used for soil erosion assessments in many areas  
81 of the world (Zapata et al. 2002; Mabit et al. 2008; Golosov et al. 2013; Alewell et al. 2014) and its feasibility for  
82 forest areas has been revealed (Garcia-Oliva et al. 1995; Porto et al. 2001; 2009; Estrany et al. 2016). The use of  
83  $^{137}\text{Cs}$  offers a great potential to provide retrospective information on medium-term average of soil loss on the basis  
84 of a single sampling without the need to disturb the system by installing measuring equipment. The  $^{137}\text{Cs}$  technique  
85 makes use of the global fallout of bomb-derived radiocaesium which occurred during a period extending from the  
86 mid 1950s to the late 1970s. In most environments, the  $^{137}\text{Cs}$  fallout reaching the land surface was rapidly adsorbed  
87 by the surface soil and its subsequent redistribution within the landscape will have occurred in association with  
88 the erosion, transport and deposition of soil and sediment particles. For forest environments, Porto et al. (2001;

89 2014) demonstrated the feasibility of the  $^{137}\text{Cs}$  approach by comparing estimates of soil erosion provided by the  
90 latter with long-term measurements of sediment yield available in small catchments afforested with eucalypt  
91 (*Eucalyptus occidentalis* E.). However, to date, no information on the relationships between  $^{137}\text{Cs}$  and parameters  
92 like canopy cover, tree species, forest vertical stratification and types of forest management are reported.

93 In this work, a set of four experimental plots in beech and Calabrian pine forest stands was established with the  
94 aim to study the relationships between different types of forest management and the observed rates of soil loss  
95 using  $^{137}\text{Cs}$ .

96

## 97 **2 Materials and methods**

### 98 2.1 Study area

99 The study area is located in Ferraina, within the Aspromonte National Park, Calabria, Southern Italy (**Fig. 1**). In  
100 this site, four rectangular plots (15 m x 20 m), with slope values ranging from 9% to 22%, were established in  
101 2016 (**Fig. 2**). The choice related to the rectangular shape of each plot (with the longer axis parallel to the flow  
102 direction) was made with the aim to compare the results of this experiment with those that can be provided by  
103 other models like RUSLE (and derived versions) that explore the same range of length and slope.

104 The forest cover consists of two Calabrian pine (*Pinus nigra laricio* Poir.) stands, with different canopy cover and  
105 living biomass amounts, and two beech (*Fagus sylvatica* L.) stands (one of which was cut in 2009). More  
106 particularly, the first two plots, namely 'Pine stand 1' and 'Pine stand 2', are covered by Pine forests (ca. 50 years  
107 old) planted in the late 1960s during a massive re-afforestation programme (ca. 150,000 ha) carried out in Calabria.  
108 The remaining two plots, namely 'Beech stand 3' and 'Beech stand 4', consist of semi-natural high Beech forests  
109 (ca. 140 years old) typical of the mountain areas of the Mediterranean basin. Beech stand 4 was substantially  
110 undisturbed by cutting activities, with the exception of minimal removal of trees in the past decades; on the  
111 contrary, Beech stand 3 was clearcut in 2009 and then left to evolve naturally.

112 A reference site with no tree coverage was also selected within an undisturbed flat area, located nearby the forested  
113 plots, in order to collect information on  $^{137}\text{Cs}$  fallout on the overall study area. The elevation of the study area  
114 ranges from 1366 to 1465 m a.s.l.. The mean value of annual rainfall, based on the data obtained at Gambarie  
115 d'Aspromonte meteorological station (38°07'36''N, 15°57'08''E - 1300 m a.s.l.) and available for the period 1931-

116 2016, is 1611 mm, with a mean value of annual temperature of 10.6 °C. The climate of the area is classified as  
117 oceanic temperate. The major soil types are characterised by a silt-loam texture (Soil Survey Staff 1993).

118

## 119 2.2 Soil sample collection for <sup>137</sup>Cs analysis

120 Soil samples were collected in 2016. A detailed sampling programme was established to provide long term data  
121 useful to estimate erosion and deposition rates according to the amount of <sup>137</sup>Cs in the soil. A total of nine replicate  
122 soil cores was collected for each plot, using a 10-cm-diameter steel core tube inserted to a depth of ca. 42 cm.  
123 More particularly, three transects aligned with the line of steepest slope were established for each plot. In the  
124 central transect, three replicate sectioned cores (each one consisting of 14 x 2 = 28 layers) were collected in order  
125 to obtain information on cesium distribution in soil. Six additional replicate bulk cores were also collected from  
126 the remaining two transects (see **Fig. 2**).

127 Even if several studies have emphasized the effect of forest canopy on fallout interception (see among the others  
128 Bunzl et al. 1995; Strebl et al. 1999; Takenaka et al. 1998), our samples were collected from small clearings under  
129 the trees to reduce this effect. It is worth noticing that the Pine trees on Plot 1 and Plot 2 were planted at the end  
130 of '60s when most of <sup>137</sup>Cs fallout had already reached the ground. At that time, the ground was similar to that of  
131 the undisturbed area selected as reference site. As a result, in these two plots, fallout interception was minimal  
132 during the period covered by the trees and the <sup>137</sup>Cs inventories are then comparable with those obtained in the  
133 reference area (see description below). In Plot 3 and Plot 4, possible fallout interception has occurred due to the  
134 longer life of the beech stands (ca. 140 years). However, in Mediterranean areas, most of the rainfall is concentrated  
135 in winter time when the deciduous species show no foliage cover. Experimental measurements available for  
136 deciduous species (see, for example, Lee 1980; Bruijnzeel and Wiersum 1987) documented values of interception  
137 around 10-15% for rainfall higher than 15 mm and for forests with uniform canopy cover. These findings, together  
138 with the sampling strategy adopted (consisting of taking samples from small gaps), have probably minimized the  
139 effect of fallout interception. However, care was also taken to avoid sampling points close to the tree trunks in  
140 order to minimize the effect of stemflow on the final <sup>137</sup>Cs inventories.

141 In order to obtain information on the <sup>137</sup>Cs reference value, a detailed soil sampling campaign was also carried out  
142 in the reference area located nearby the study plots (elevation = 1400 m a.s.l.). In this case, four separate sectioned  
143 cores were collected within a large forest gap, using the same procedure as employed for the sectioned cores

144 collected in the study plots. This sampling strategy was adopted to account for the micro-scale variability of the  
 145 atmospheric fallout (see Porto and Walling 2013).

146 After collection, each core was transported in the laboratory and pre-treated for  $^{137}\text{Cs}$  measurements. A total of  
 147 384 soil samples (336 from the sectioned cores and 48 bulk cores) were collected for the study plots while 120  
 148 samples were obtained for the reference area. All the samples were oven dried at 105 °C for 48 h, disaggregated,  
 149 dry sieved to separate the <2 mm fraction and packed in plastic pots or petri dishes for determination of its  $^{137}\text{Cs}$   
 150 activity by gamma spectroscopy at the University Mediterranea of Reggio Calabria. The gamma-ray spectrometry  
 151 equipment used in this study consists of 2 Canberra p-type HPGe detectors, model GX4020. Each detector has  
 152 45.6% of relative efficiency with a resolution of 1.1 keV at 122 keV and 2.0 keV at 1.33 MeV and it works coupled  
 153 to a Desktop Spectrum Analyzer DSA-1000 Canberra multichannel analyzer. The spectral analysis is performed  
 154 using the Canberra Genie 2000 software package. Each detector has been characterized to permit the efficiency  
 155 calibration by the Canberra's LabSOCS (Laboratory SOurceless Calibration Software) code that performs  
 156 mathematical efficiency calibrations of Ge detectors, without any use of radioactive sources by the laboratory user.  
 157 The energy calibration was obtained using a certified multigamma source with a wide energy range (42.8-1274.5  
 158 keV). Also, a further validation phase was performed using the activity concentration for  $^{137}\text{Cs}$  of several standard  
 159 materials of different geometry to cover the specific range of energy of this radionuclide. Count times in the  
 160 detectors were typically approximately 80000 s and the  $^{137}\text{Cs}$  activities were obtained from the counts at 662 keV.  
 161 In order to convert  $^{137}\text{Cs}$  measurements into soil erosion and deposition estimates, the diffusion and migration  
 162 model (DMM) originally proposed by Walling and He (1999) and refined by Porto et al. (2003), was used. The  
 163 DMM simulates the time evolution of  $^{137}\text{Cs}$  within a soil profile based on the atmospheric fallout and on its post-  
 164 depositional redistribution. Porto et al. (2003) reported the following equation to interpret the activity of  $^{137}\text{Cs}$   
 165 within the soil profile (see also Lindstrom and Boersma 1971; Officer and Lynch 1982; Walling and He 1999):

$$\begin{aligned}
 C(x, t, t') = & e^{-\lambda(t-t')} \int_0^{\infty} \frac{I(t')}{H} e^{-\frac{y}{H}} \left\{ e^{\frac{V(x-y)}{2D} - \frac{V^2(t-t')}{4D}} \left[ e^{-\frac{(x+y)^2}{4D(t-t')}} + e^{-\frac{(x-y)^2}{4D(t-t')}} \right] \times \right. \\
 & \left. \times \frac{1}{\sqrt{4\pi D(t-t')}} - \frac{V}{2D} e^{\frac{Vx}{D}} \operatorname{erfc} \left[ \frac{x+y+V(t-t')}{\sqrt{4D(t-t')}} \right] \right\} dy
 \end{aligned} \tag{1}$$

167 where:

168  $C(x, t, t')$ , expressed in  $\text{Bq kg}^{-1}$ , is the  $^{137}\text{Cs}$  activity related to the mass depth  $x$  and time  $t'$ .

169  $D$  ( $\text{kg}^2 \text{m}^{-4} \text{yr}^{-1}$ ) represents the time-averaged estimate of the diffusion coefficient;  
 170  $V$  ( $\text{kg m}^{-2} \text{yr}^{-1}$ ) is the downward migration rate;  
 171  $H$  ( $\text{kg m}^{-2}$ ) indicates the relaxation mass depth i.e. the  $^{137}\text{Cs}$  initial distribution along the soil profile following the  
 172 atmospheric fallout;  
 173  $\lambda$  ( $= 0.023 \text{yr}^{-1}$ ) is the constant of radioactive decay for  $^{137}\text{Cs}$ ;  
 174  $x$  ( $\text{kg m}^{-2}$ ) is the soil mass depth measured from the soil surface downwards;  
 175  $t$  (yr) is the time elapsed since the first fallout;  
 176  $I(t')$ , expressed in ( $\text{Bq m}^{-2} \text{yr}^{-1}$ ), indicates the  $^{137}\text{Cs}$  atmospheric flux at time  $t'$ .  
 177  $\text{erfc}(u)$  is the error-function complement defined as (Crank 1975):

$$178 \quad \text{erfc}(u) = \frac{2}{\sqrt{\pi}} \int_u^{\infty} e^{-y^2} dy \quad (2)$$

179

180 Taking account of a continuous input  $I(t')$ , the  $^{137}\text{Cs}$  concentration distribution  $C(x,t)$  ( $\text{Bq kg}^{-1}$ ) in the soil profile  
 181 at time  $t$  can be obtained by integrating  $C(x,t,t')$  over time  $t'$  (Walling and He 1993):

$$182 \quad C(x,t) = \int_0^t C(x,t,t') dt \quad (3)$$

183 The reason of this choice is related to the meaningful results obtained with the use of DMM in southern Italy (see  
 184 Porto et al. 2003; 2014) and to the visual inspection of the profiles reported in **Fig. 3** and **Fig. 4** that show a peak  
 185 below the soil surface

186

### 187 2.3 Structural analysis of the study plots

188 To better represent the forest structure in the plots and to correlate soil erosion estimates provided by  $^{137}\text{Cs}$  with  
 189 the type of forest management in the study area, dendrometric measurements were carried out in the same plots  
 190 with the exception of Beech stand 3 where no trees are available. All the trees in the plots were georeferenced and  
 191 measurements of height, and diameter have been carried out. Data were then processed to calculate the values of  
 192 the Basal Area ( $\text{m}^2 \text{ha}^{-1}$ ), Volume ( $\text{m}^3 \text{ha}^{-1}$ ), Number of plants per plot, and Number of plants per hectare. Moreover,  
 193 in order to represent the vertical and horizontal forest structure within the study plots, measures on tree spatial  
 194 distribution, canopy insertion height and tree canopy projection on the forest soil were also carried out. Data were



195 then processed through the Stand Visualization System software (USDA, Forest Service) to show the tree spatial  
196 distribution for each plot. In addition, hemispherical photos using a fish eye lens were collected and processed  
197 with the GLA (Gap Light Analyzer) software for calculating the canopy cover and the leaf area index (LAI).

198

### 199 **3 Results**

#### 200 3.1 $^{137}\text{Cs}$ inventories and depth distributions at the reference site and study plots and soil erosion estimates

201 The four sectioned cores collected within the reference area produced 120 soil samples (2-cm increment). The  
202 matching depth increments were bulked prior to gamma assay, and a representative estimate of the local reference  
203 inventory and its depth distribution were obtained. This profile, reported in **Fig. 3** together with the fitting provided  
204 by the DMM, is typical of an undisturbed site (see Porto et al. 2003). It shows about 90% of the total inventory  
205 occurring in the top 15 cm, a peak in activity ca. 6 cm below the soil surface, and a sharp exponential decline in  
206 activity below this depth. This profile shows a reference inventory of 5949 Bq m<sup>-2</sup>, in agreement with what found  
207 in other areas of South Italy with similar annual rainfall (see Porto and Walling 2012). As mentioned above, the  
208 profile was built on the matching depth increments in order to cover the spatial variability of the atmospheric  
209 fallout. However, we considered a 10% uncertainty around this value (see Table 1) to account for the measurements  
210 error due to the equipment. The values of  $^{137}\text{Cs}$  inventory associated with the samples collected from the plots are  
211 reported in **Table 1** while the  $^{137}\text{Cs}$  depth distributions associated with each plot are illustrated in **Fig. 4**. The four  
212  $^{137}\text{Cs}$  depth distributions in **Fig. 4**, one for each plot, indicate different inventory values but they show a similar  
213 shape that conforms to that expected for uncultivated soils.

214 Information on the  $^{137}\text{Cs}$  inventory values for the study plots, provided in **Table 1**, indicates that 29 out of 36  
215 sampling sites (including the profiles in **Fig. 4**) show inventory values lower than the reference value pointing out  
216 evidence of soil erosion within the plots. Only 7 points documented evidence of deposition with  $^{137}\text{Cs}$  inventories  
217 higher than the reference value. A mean value of 4689 Bq m<sup>-2</sup> (lower than the reference inventory), obtained from  
218 the 36 single points, showed that erosion was the dominant process during the time span (ca. 60 years) covered by  
219 the  $^{137}\text{Cs}$  measurements.

220 Information on the corresponding estimates of soil loss provided by the DMM is also reported in **Table 1** for each  
221 plot.

222

### 223 3.2 Structural data of the study plots

224 Data obtained from the structural surveys are listed in **Table 2**. Pine stand 1, Pine stand 2, and Beech stand 4  
225 showed respectively a mean diameter of 32.31 cm, 33.27 cm and 36 cm. The same stands showed volume values  
226 of 699 m<sup>3</sup> ha<sup>-1</sup>, 1589 m<sup>3</sup> ha<sup>-1</sup> and 1080 m<sup>3</sup> ha<sup>-1</sup> while the number of trees per hectare was 866, 1500 and 933,  
227 respectively. The tree canopy cover determined with the use of hemispherical photos and the GLA software was  
228 52% for Pine stand 1, 63% for Pine stand 2 and 51% for Beech stand 4. The corresponding values of the leaf area  
229 index (LAI) were 0.79 (m<sup>2</sup> m<sup>-2</sup>), 1.13 (m<sup>2</sup> m<sup>-2</sup>) and 0.80 (m<sup>2</sup> m<sup>-2</sup>), respectively.

230

### 231 4 Discussion

232 The results reported in **Table 1** show different values of <sup>137</sup>Cs inventories. The significance of these differences  
233 was checked, preliminarily, using the Friedman test (see Kanji 1993). The resulting statistics were always higher  
234 than the critical value at the 0.05 level of significance, indicating that there were significant difference between  
235 the 4 empirical distributions of <sup>137</sup>Cs values associated with the plots.

236 The <sup>137</sup>Cs measurements carried out in the 9 sampling points selected in each plot provided an estimate of the  
237 average soil redistribution rates for the period extending from the commencement of <sup>137</sup>Cs fallout in the mid-1950s  
238 to the present. As explained above, the use of these measurements was based on the comparison between the  
239 radionuclide reference value obtained in the reference area and the <sup>137</sup>Cs inventories measured in the 9 single points  
240 for each plot. Most of the latter inventories (29 out of 36) were lower than the reference value, indicating that soil  
241 erosion was a dominant process during the last ca. 60 years. The mean value of the erosion rates, reported in **Tab.**  
242 **1** for each plot, range from 0.38 t ha<sup>-1</sup> yr<sup>-1</sup> to 1.34 t ha<sup>-1</sup> yr<sup>-1</sup>. These values are generally lower than the annual mean  
243 values considered as 'issue of concern' by the scientific literature. Verheijen et al. (1999), for example, even when  
244 dust deposition is included in soil formation rates, reported an upper limit of tolerable soil erosion of ca. 1.4 t ha<sup>-1</sup>  
245 yr<sup>-1</sup>. These findings support strongly the hypothesis that forests play a key role in regulating the runoff and soil  
246 erosion, due to the protection offered by the canopy cover and to their capability of improving the absorption  
247 capacity of soils. In fact, both these functions are useful to reduce the overland flow and the water erosion risks  
248 related. However, some differences between the four forest types selected in this study must be recognised. In  
249 order to facilitate the comparison between the four treatments, a spatial visualization of the trees, obtained with  
250 the SVS software, is provided in **Fig. 5A-D**. The corresponding spatial distribution of soil erosion rates was also  
251 created, using a kriging interpolation procedure, and is depicted in **Fig. 5E-H**.

252 A first comparison can be made between Plot 1 and Plot 2, having the same forest type (Pine stand) but with  
253 different forest cover and biomass. Pine stand 1, characterised by a canopy cover of 52%, shows a mean value of  
254 soil erosion equal to  $1.16 \text{ t ha}^{-1} \text{ yr}^{-1}$  that is higher than that documented by Pine stand 2 (only  $0.26 \text{ t ha}^{-1} \text{ yr}^{-1}$ ) where  
255 the canopy cover is 63%. The higher value of soil erosion in Pine stand 1 could also be due to a minor tree density  
256 ( $866 \text{ trees ha}^{-1}$ ) compared to that ( $1500 \text{ trees ha}^{-1}$ ) measured in Pine stand 2 (see also Fig. 5<sub>A,B</sub>). A higher tree  
257 density in fact, enhances the soil protection due, for example, to a stronger root system and a larger surface taken  
258 up by the tree canopy that intercepts a higher amount of rainfall and limits the raindrop impact on the ground (see  
259 Chapman 1948). The different forest covers and tree density currently found in both pine stands are part of the  
260 same type of silvicultural treatment. These differences are probably due to micro-variability (e.g. small disturbances  
261 and stand dynamic evolution) in that area (Gray and Spies 1996). Anyway, the management of the stand in the  
262 past years preserved the protective role of the trees against soil erosion processes. These findings emphasise the  
263 conclusion that an increase in forest cover and biomass improves soil protection. The pattern of soil erosion rates  
264 depicted in Fig. 5<sub>E,F</sub> clearly delineates the areas with the highest rates of soil loss within the plots. A close  
265 correspondence with the lower values of canopy cover can be observed (see Fig. 5<sub>A,B</sub>) and this supports the above  
266 conclusion.

267 A second important comparison can be observed between Plot 1 and Plot 4 having similar canopy cover (52% and  
268 51%) but characterised by two different forest species (Pine and Beech, respectively). The mean value of soil  
269 erosion in Beech stand 4 ( $0.68 \text{ t ha}^{-1} \text{ yr}^{-1}$ ) is lower than that documented in Pine stand 1 and seems to suggest a  
270 better protection against soil erosion offered by the former. A possible explanation of this result can be related to  
271 the greater canopy cover capacity expected for deciduous species than for conifers, as documented by other authors  
272 (see among the others, Helvey and Patric 1965; Zinke 1967). Another possible reason for these lower values of  
273 soil erosion rates can be ascribed to the Beech root system that is generally shallow and superficial, with large  
274 roots spreading out in all directions. Conversely, the Pine root system is relatively deeper and does not offer the  
275 same protection against erosion of the first soil layers. However, the role of the canopy cover in protecting the soil  
276 from erosion is confirmed by the spatial pattern of soil erosion rates depicted in Fig. 5<sub>H</sub>. In fact, a comparison with  
277 the spatial visualization of the trees in Fig. 5<sub>D</sub> shows, again, a close correspondence of the areas with higher erosion  
278 rate with the lower values of canopy cover.

279 A last important comparison can be made between the Beech stand in Plot 4 and the forest system in Plot 3,  
280 originally covered by a Beech stand that was clearcut in 2009. In this case, it was possible to explore the effect  
281 reflected by the clearcutting in terms of soil loss from this area. The mean value of soil erosion rate for the Beech

282 stand 3 is  $1.34 \text{ t ha}^{-1} \text{ yr}^{-1}$ , almost double that from Beech stand 4. This result is clearly not unexpected because the  
283 temporary lack of canopy cover occurred during the last 7 years may have affected soil properties and this resulted  
284 in significant increase of soil loss in recent periods. However, it must be recognised that the last 6-7 years following  
285 the clearcutting are characterised by the occurrence of very severe rainfall events that coincided with the absence  
286 of vegetation in this area and may have affected strongly the rate of soil loss in the same period. Although no direct  
287 measurements of soil erosion are available for the recent years, an attempt to reconstruct the trend of soil loss using  
288 the rainfall erosivity factor (Wischmeier and Smith 1978) can be made. This trend is depicted in **Fig. 6** for  
289 Gambarie meteo station located in the vicinity of the study site. The dataset of the 30-min rainfall is available from  
290 1991 to date. The clearcutting occurred in October 2009 and **Fig. 6** indicate that for the set of storm events occurred  
291 from that period to the sampling date, the mean value of the R-factor ( $R_m = 4473 \text{ MJ ha}^{-1} \text{ mm}^{-1} \text{ h}^{-1}$ ) was significantly  
292 greater than that related to the period 1991-2008 ( $R_m = 2635 \text{ MJ ha}^{-1} \text{ mm}^{-1} \text{ h}^{-1}$ ). The increase is particularly marked  
293 for the events that occurred in 2015, prior to the sampling campaign. Similar trends of the R-factor, with a general  
294 increase during the last decade, have been also documented by Capra et al. (2017) for other stations located in the  
295 same region. The higher values of the R-factor, combined with the tree cutting showed a general increase of soil  
296 erosion even in other areas, emphasizing the importance of vegetation in protecting the soil (see Porto et al. 2009).  
297 However, further measurements are needed during the next years to establish if the effect of the clearcutting might  
298 be mitigated while the new vegetation will take place.

299

## 300 **5 Conclusions**

301 The overall results obtained in this experiment demonstrated, first of all, the ability of  $^{137}\text{Cs}$  as a tracer technique  
302 to predict soil erosion rates. Based on the  $^{137}\text{Cs}$  measurements, minimum values of soil loss ( $0.26 \text{ t ha yr}^{-1}$ ) are  
303 documented in areas covered by Pine stand with higher canopy cover and biomass (Plot 2), evidencing the  
304 protective effect provided by forests against soil erosion. The experiment demonstrated that when canopy cover is  
305 lower and discontinuous, as in the two cases described in Plot 1 and Plot 4, the  $^{137}\text{Cs}$  measurements documented  
306 higher values of soil loss, equal to  $1.16 \text{ t ha}^{-1} \text{ yr}^{-1}$ , and  $0.68 \text{ t ha}^{-1} \text{ yr}^{-1}$ , respectively. These findings indicate that  
307 when afforestation programmes or new plantations activities are planned, but also during the silvicultural  
308 treatments, it is necessary to reduce the occurrence of large gaps among the forest cover in order to reduce soil  
309 erosion. The effectiveness of canopy is also evident in the uncovered area (Plot 3) where the original Beech stand  
310 was clearcut in 2009. In this case, the mean rate of soil loss provided by the  $^{137}\text{Cs}$  measurements was  $1.34 \text{ t ha}^{-1}$

311 yr<sup>-1</sup>, almost double that in the area (Plot 4) where the same forest type was maintained undisturbed. Although the  
312 clearcutting operations occurred in a period during which the rainfall erosivity was the highest in the last 25 years,  
313 the experiment indicates that care must be taken when new silviculture treatments are planned. These findings are  
314 in agreement with what documented by other authors in similar environments but further work is necessary to  
315 establish the effectiveness of <sup>137</sup>Cs measurements in different forest contexts.

316

317 **Acknowledgements** This study was supported by the Coordinated Research Project (CRP) D1.50.17 within the  
318 framework of the International Atomic Energy Agency (IAEA). The authors are also indebted to the ARPACAL  
319 for providing rainfall data used in this study.

320

## 321 **References**

- 322 Alcamo J, Flörke M, Märker M (2007) Future long-term changes in global water resources driven by socio-  
323 economic and climatic changes. *Hydrolog Sci J* 52(2):247-275. doi.org/10.1623/hysj.52.2.247
- 324 Alewell C, Meusburger K, Juretzko G, Mabit L, Ketterer ME (2014) Suitability of <sup>239+240</sup>Pu and <sup>137</sup>Cs as tracers  
325 for soil erosion assessment in mountain grasslands. *Chemosphere* 103:274-280. doi:  
326 10.1016/j.chemosphere.2013.12.016
- 327 Bagarello V, Ferro V, Giordano G (2010) Testing alternative erosivity indices to predict event soil loss from bare  
328 plots in Southern Italy. *Hydrol Process* 24(6):789-797. doi: 10.1002/hyp.7538
- 329 Bosch JM, Hewlett JD (1982) A review of catchment experiments to determine the effect of vegetation changes  
330 on water yield and evapotranspiration. *J Hydrol* 55(1-4):3-23. doi.org/10.1016/0022-1694(82)90117-2
- 331 Bunzl K, Kracke W, Schimmack W (1995) Migration of fallout <sup>239+240</sup>Pu, <sup>241</sup>Am and <sup>137</sup>Cs in the various horizons  
332 of a forest soil under pine. *J Environ Radioactiv* 28: 17-34.
- 333 Bruijnzeel LA, Wiersum KF (1987) Rainfall interception by a young *Acacia auriculiformis* (A. Cunn) plantation  
334 forest in West Java, Indonesia: application of gash's analytical model. *Hydrol Process* 1, 309-319.
- 335 Capra A, Porto P, La Spada C. (2017) Long-term variation of rainfall erosivity in Calabria (Southern Italy). *Theor*  
336 *Appl Climatol* 128, Issue 1–2, pp 141–158. DOI 10.1007/s00704-015-1697-2.
- 337 Chapman G (1948) Size of raindrops and their striking force at the soil surface in a red pine plantation. *Eos Trans.*  
338 *AGU* 29(5): 664–670, doi:10.1029/TR029i005p00664.

339 Conacher AJ, Sala M (1998) Land degradation in Mediterranean environments of the world: nature and extent,  
340 causes and solutions. John Wiley and Sons Ltd, Australia

341 Crank J (1975) The Mathematics of Diffusion. 2nd ed. Clarendon Press, pp. 414.

342 Elliot WJ, Page-Dumroese D, Robichaud PR (1999) The effects of forest management on erosion and soil  
343 productivity. Proceedings of the Symposium on Soil Quality and Erosion Interaction, Keystone, CO, July 7,  
344 1996. Ankeney, IA: Soil and Water Conservation Society, p 195

345 Estrany J, López-Tarazón JA, Smith HG (2016) Wildfire effects on suspended sediment delivery quantified using  
346 fallout radionuclide tracers in a Mediterranean catchment. *Land Degrad Dev* 27:1501-1512. DOI:  
347 10.1002/ldr.2462

348 Evans R, Boardman J (2016) The new assessment of soil loss by water erosion in Europe. Panagos P. et al. 2015.  
349 *Environmental Science & Policy* 54 438–447- a response. *Environ. Sci. Pol.* 58: 11–15.

350 Evans R, Collins AL, Foster IDL, Rickson RJ, Anthony SG, Brewer T, Deeks L, Newell-Price JP. Truckell IG,  
351 Zhang Y. (2016) Extent, frequency and rate of water erosion of arable land in Britain – benefits and  
352 challenges for modelling. *Soil Use Manag.* 32 (Supplement S1): 149–161.

353 Garcia-Oliva F, Martinez Lugo R, Maass JM (1995) Long-term net soil erosion as determined by <sup>137</sup>Cs  
354 redistribution in an undisturbed and perturbed tropical deciduous forest ecosystem. *Geoderma* 68:135–147.  
355 doi.org/10.1016/0016-7061(95)00030-R

356 Golosov VN, Belyaev V, Markelov MV (2013) Application of Chernobyl-derived <sup>137</sup>Cs fallout for sediment  
357 redistribution studies: lessons from European Russia. *Hydrol Process* 27(6):781-794. DOI:  
358 10.1002/hyp.9470.

359 Gray AN, Spies TA (1996) Gap size, within-gap position and canopy structure effects on conifer seedling  
360 establishment. *J Ecol* 8:635-645. doi: 10.2307/2261327

361 Hartanto H, Prabhu R, Widayat AS, Asdak C (2003) Factors affecting runoff and soil erosion: plot-level soil loss  
362 monitoring for assessing sustainability of forest management. *Forest Ecol Manag* 180(1):361-374.  
363 doi.org/10.1016/S0378-1127(02)00656-4

364 Helvey JD, Patric JH (1965) Canopy and litter interception of rainfall by hardwoods of eastern United States.  
365 *Water Resour Res* 1:193-206. doi: 10.1029/WR001i002p00193

366 Kanji GK (1993) 100 Statistical tests. Sage publications, London, Newbury Park, New Delhi

367 Lee R (1980) Forest hydrology. Columbia University Press, New York, pp 1-349

368 Lindstrom FT, Boersma L (1971) A theory on the mass transport of previously distributed chemicals in a water-  
369 saturated sorbing porous medium. *Soil Sci.* 111: 192-199

370 Mabit L, Benmansour M, Walling DE (2008) Comparative advantages and limitations of the fallout radionuclides  
371  $^{137}\text{Cs}$ ,  $^{210}\text{Pb}_{\text{ex}}$  and  $^7\text{Be}$  for assessing soil erosion and sedimentation. *J Environ Radioactiv* 99:1799-1807.  
372 doi.org/10.1016/j.jenvrad.2008.08.009

373 Miura S, Yoshinaga S, Yamada T (2003) Protective effect of floor cover against soil erosion on steep slopes  
374 forested with *Chamaecyparis obtusa* (hinoki) and other species. *J Forest Res-JPN* 8(1):27-35.  
375 doi.org/10.1007/s103100300003

376 Montanarella L. (2007) Trends in Land Degradation in Europe. In: Sivakumar MVK, Ndiang'ui N (eds) *Climate  
377 and Land Degradation. Environmental Science and Engineering (Environmental Science)*, Springer, Berlin,  
378 Heidelberg. DOI 10.1007/978-3-540-72438-4\_5, pp 83-104

379 Moore R, Wondzell SM (2005) Physical hydrology and the effects of forest harvesting in the Pacific Northwest:  
380 a review. *J Am Water Resour Ass* 41(4):763-784. doi: 10.1111/j.1752-1688.2005.tb03770.x

381 Morgan RPC (1992) Soil erosion in the northern countries of the European Community. In: *EIW Workshop:  
382 elaboration of a framework of a code of good agricultural practices*, Brussels, pp 21-22

383 Officer CB, Lynch DR (1982) Interpretation procedures for the determination of sediment parameters from time-  
384 dependent flux inputs. *Earth and Planetary Science Letters* 61: 55-62

385 Ollesch G, Vacca A (2002) Influence of time on measurement results of erosion plot studies. *Soil Till Res* 67(1):23-  
386 39. doi.org/10.1016/S0167-1987(02)00029-6

387 Pennock DJ, Van Kessel C (1997) Clear-cut forest harvest impacts on soil quality indicators in the mixedwood  
388 forest of Saskatchewan, Canada. *Geoderma* 75(1-2):13-32. doi.org/10.1016/S0016-7061(96)00075-4

389 Porto P, Walling DE (2012a) Validating the use of  $^{137}\text{Cs}$  and  $^{210}\text{Pb}_{\text{ex}}$  measurements to estimate rates of soil loss  
390 from cultivated land in southern Italy. *J Environ Radioactiv* 106:47-57.  
391 doi.org/10.1016/j.jenvrad.2011.11.005

392 Porto P, Walling DE (2012b) Using plot experiments to test the validity of mass balance models employed to  
393 estimate soil redistribution rates from  $^{137}\text{Cs}$  and  $^{210}\text{Pb}_{\text{ex}}$  measurements. *Appl Radiat Isotopes* 70:2451-2459.  
394 doi.org/10.1016/j.apradiso.2012.06.012

395 Porto P, Walling DE, Alewell C, Callegari G, Mabit L, Mallimo N, Meusburger K, Zehringer M. (2014) Use of a  
396  $^{137}\text{Cs}$  re-sampling technique to investigate temporal changes in soil erosion and sediment mobilisation for a  
397 small forested catchment in southern Italy. *J Environ Radioactiv* 138:137-148.  
398 doi.org/10.1016/j.jenvrad.2014.08.007

399 Porto P, Walling DE, Callegari G (2009) Investigating the effects of afforestation on soil erosion and sediment  
400 mobilisation in two small catchments in Southern Italy. *Catena* 79:181-188.  
401 doi.org/10.1016/j.catena.2009.01.007

402 Porto P, Walling DE, Callegari G (2013) Using  $^{137}\text{Cs}$  and  $^{210}\text{Pb}_{\text{ex}}$  measurements to investigate the sediment budget  
403 of a small forested catchment in southern Italy. *Hydrol Process* 27(6):795-806. doi: 10.1002/hyp.9471

404 Porto P, Walling DE, Callegari G, Catona F (2006) Using fallout lead-210 measurements to estimate soil erosion  
405 in three small catchments in southern Italy. *Water Air Soil Poll: Focus* 6:657-667. doi.org/10.1007/s11267-  
406 006-9050-5

407 Porto P, Walling DE, Ferro V, Di Stefano C (2003) Validating erosion rate estimates provided by caesium-137  
408 measurements for two small forested catchments in Calabria, southern Italy. *Land Degrad Dev* 14:389-408.  
409 doi: 10.1002/ldr.561

410 Porto P, Walling DE, Ferro V (2001) Validating the use of caesium-137 measurements to estimate soil erosion  
411 rates in a small drainage basin in Calabria, southern Italy. *J Hydrol* 248(1):93-108. doi.org/10.1016/S0022-  
412 1694(01)00389-4

413 Reich P, Eswaran H, Beinroth F (2000) *Global Dimensions of Vulnerability to Wind and Water Erosion*. USDA,  
414 Washington

415 Sanchis MP, Torri D, Borselli L, Poesen J (2008) Climate effects on soil erodibility. *Earth Surf Proc Land*  
416 33(7):1082-1097. doi: 10.1002/esp.1604

417 Soil Survey Staff (1993) *Keys to Soil Taxonomy*, 10th ed. USDA-Natural Resources Conservation Service,  
418 Washington, DC

419 Strebl F, Gerzabek MH, Bossew P, Kienzl K (1999) Distribution of radiocaesium in an Austrian forest stand. *Sci.*  
420 *Total Environ.* 226: 75-83

421 Takenaka C, Onda Y, Hamajima Y (1998) Distribution of cesium-137 in Japanese forest soils: Correlation with  
422 the contents of organic carbon. *Sci. Total Environ.* 222: 193-199

423 Verheijen FGA, Jones RJA, Rickson RJ, Smith CJ (2009) Tolerable versus actual soil erosion rates in Europe.  
424 *Earth-Science Reviews* 94: 23–38

425 Walling DE, He Q (1999) Improved models for estimating soil erosion rates from cesium-137 measurements. *J*  
426 *Environ Qual* 28(2):611-622. doi:10.2134/jeq1999.00472425002800020027x

427 Wischmeier WH, Smith DD (1978) *Predicting rainfall erosion losses - a guide to conservation planning*.  
428 *Agriculture Handbook No. 537*, U.S. Govt. Printing Office: Washington, DC



- 429 Zanchi C (1988) Soil loss and seasonal variation of erodibility in two soils with different texture in the Mugello  
430 valley in Central Italy. *Catena Supplement*, 12(1):167-174
- 431 Zapata F, Garcia-Agudo E, Ritchie JC, Appleby PG (2002) Introduction. In: Zapata F (ed) *Handbook for the*  
432 *Assessment of Soil Erosion and Sedimentation Using Environmental Radionuclides*. Kluwer, Dordrecht, pp  
433 1–13
- 434 Zinke PJ (1967) Forest interception studies in the United States. In: W.E. Sopper and H.W. Lull eds. *International*  
435 *Symposium on Forest Hydrology*, New York, Pergamon Press
- 436
- 437

438 Table 1. <sup>137</sup>Cs inventories for the reference area and the study plots, and calculated values of soil redistribution  
 439 rates (negative values indicate erosion).

	Reference inventories		Inventories within the plots			Soil redistribution rates	
	Mean (Bq m <sup>-2</sup> )	Range (10% uncertainty) (Bq m <sup>-2</sup> )	Mean (Bq m <sup>-2</sup> )	Range (Bq m <sup>-2</sup> )	St. Dev. (Bq m <sup>-2</sup> )	Mean (t ha <sup>-1</sup> yr <sup>-1</sup> )	Range (t ha <sup>-1</sup> yr <sup>-1</sup> )
Pine stand 1	5949	5354-6544	4185	1897- 10943	2853	-1.20	-2.6 – 3.16
Pine stand 2			5609	3309- 10211	2147	-0.26	-1.7 – 2.68
Beech stand 3			3910	1374-6594	1586	-1.34	-3.0 – 0.41
Beech stand 4			4910	2845-7267	1399	-0.68	-2.0 – 0.84

440

441

442

443 Table 2. Dendrometric values obtained for each plot

Plot	Mean DBH (cm)	Mean H (m)	Basimetric area (m <sup>2</sup> ha <sup>-1</sup> )	Volume (m <sup>3</sup> ha <sup>-1</sup> )	No. of trees per hectare	Canopy cover (%)	LAI (m <sup>2</sup> m <sup>-2</sup> )
Pine stand 1	32.3	19.9	74.1	698.9	867	52	0.79
Pine stand 2	33.3	24.7	138.9	1589.9	1500	63	1.13
Beech stand 4	36.1	22.8	102.6	1080.4	933	51	0.80

444

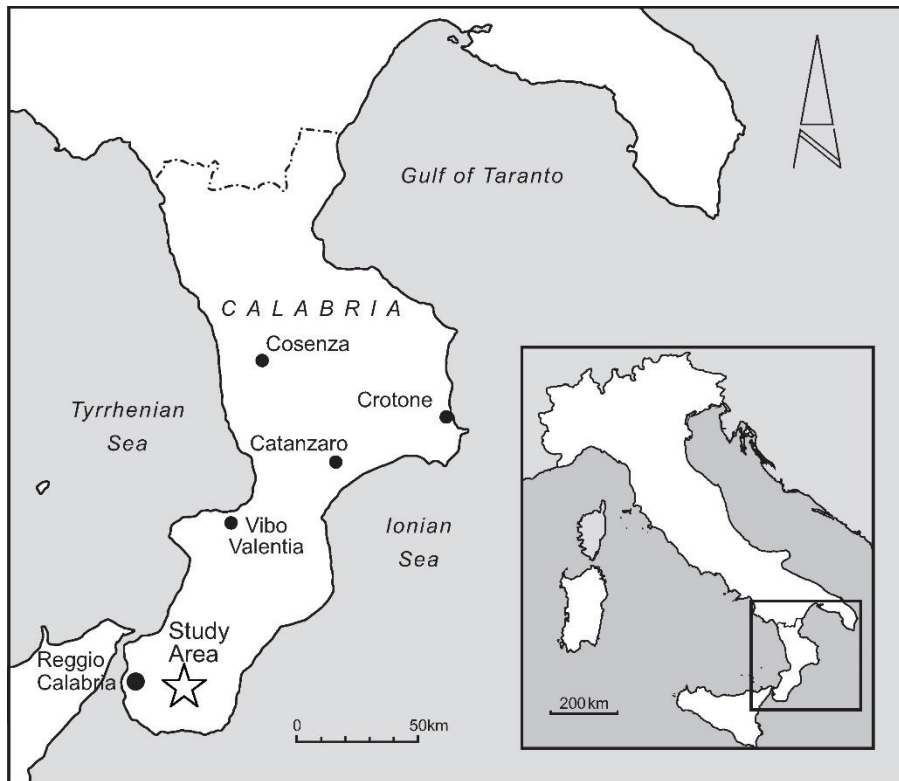
445

446

447 **Figure**

448

449



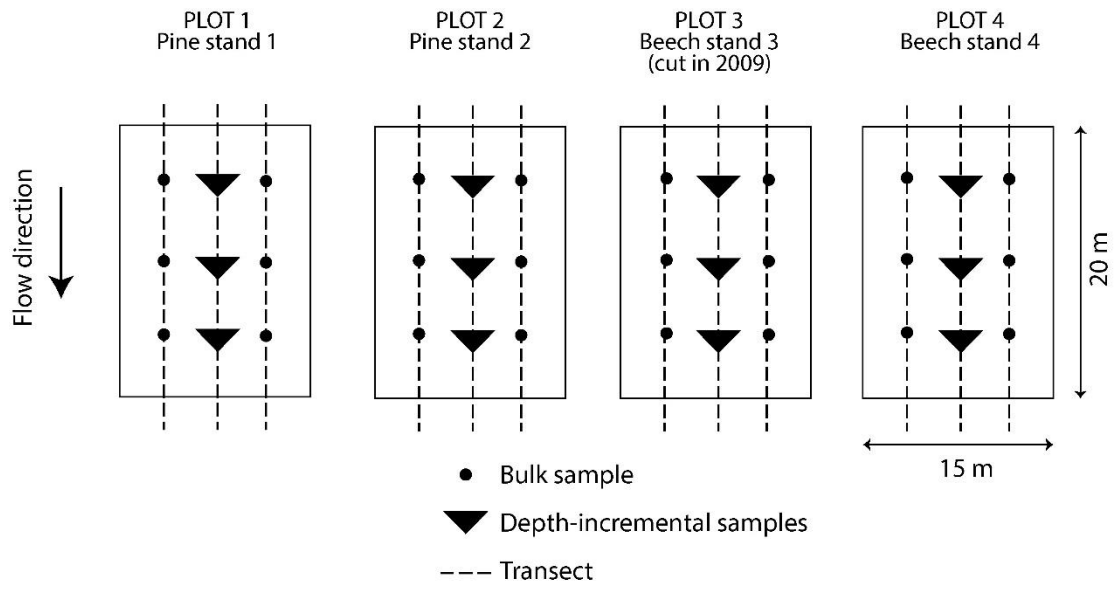
450

451 **Fig. 1** The study area

452

453

454



455

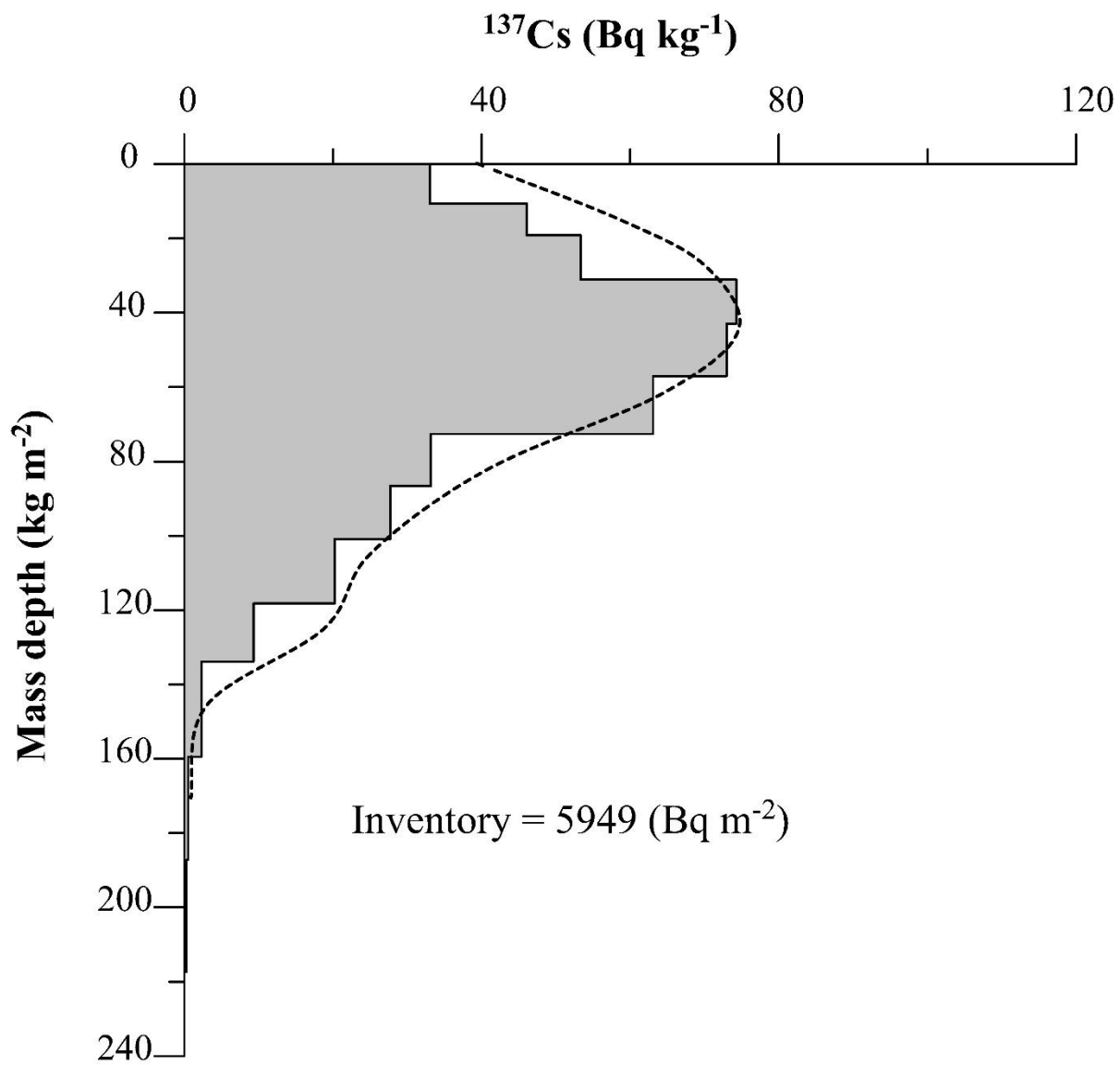
456 **Fig. 2** The experimental plots and the sampling locations

457

458

459

460



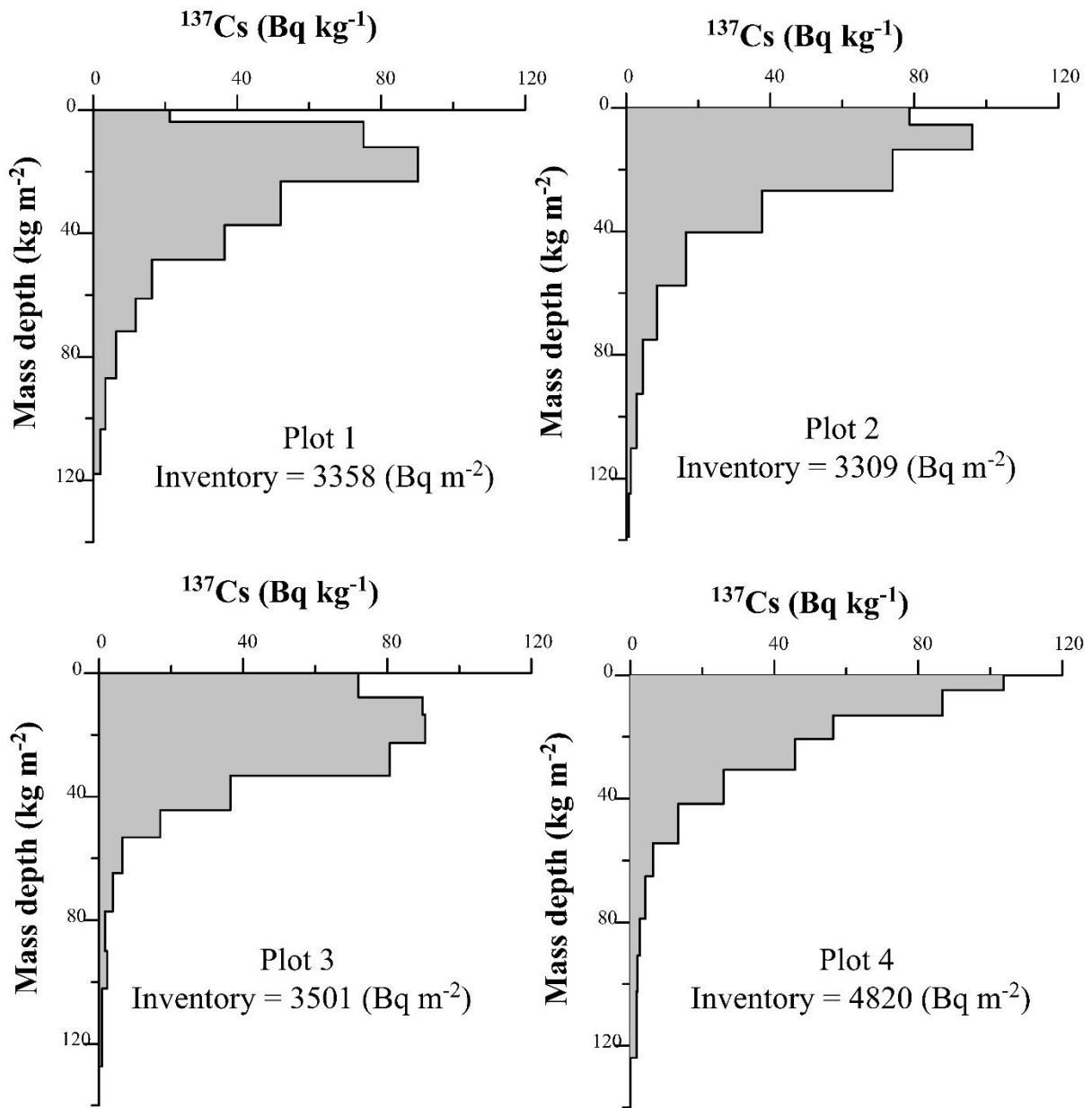
461

462 **Fig. 3**  $^{137}\text{Cs}$  inventory and depth distribution in the reference area

463

464

465



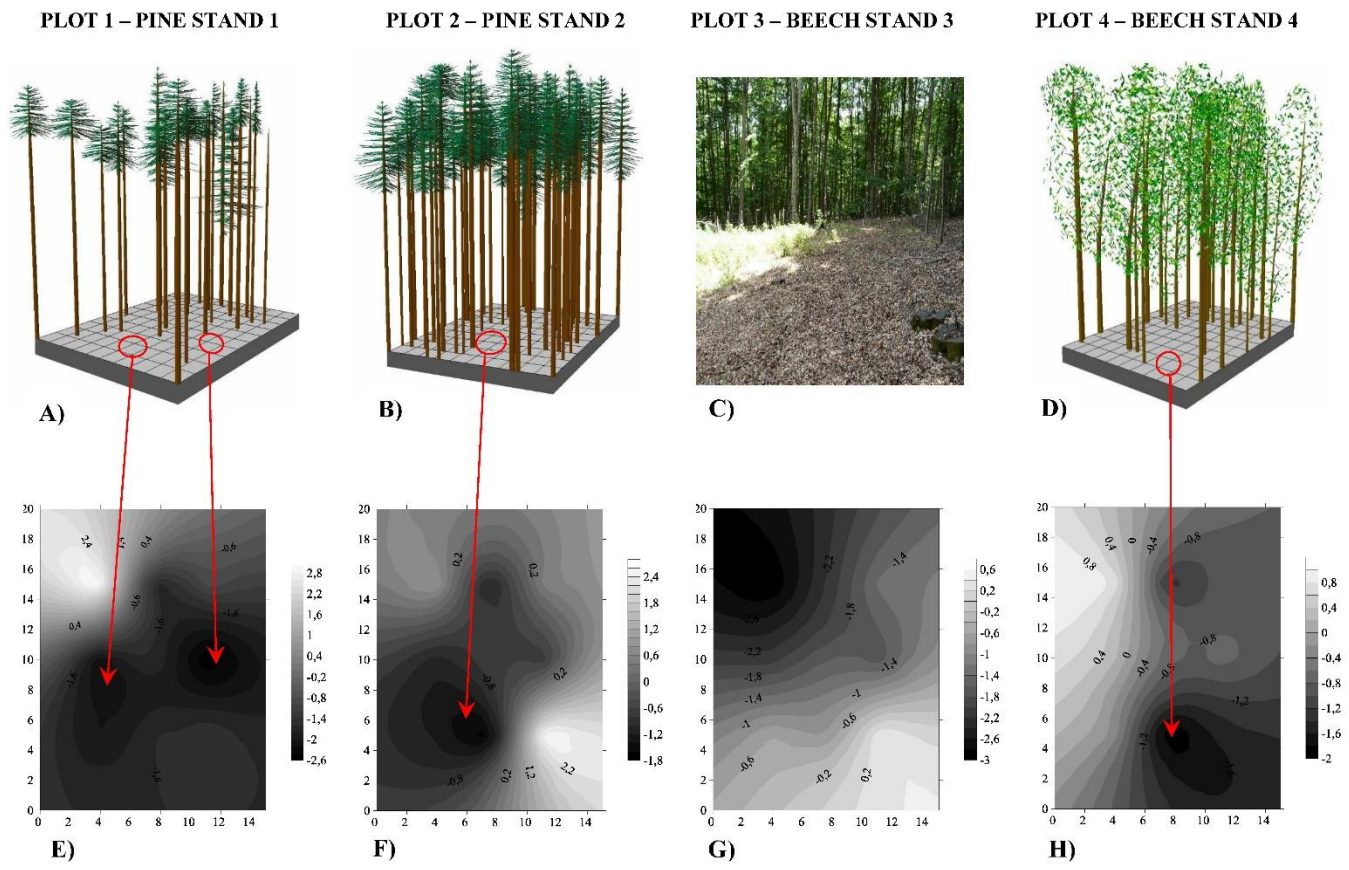
466

467 **Fig. 4** <sup>137</sup>Cs inventory and depth distribution within the study plots

468

469

470



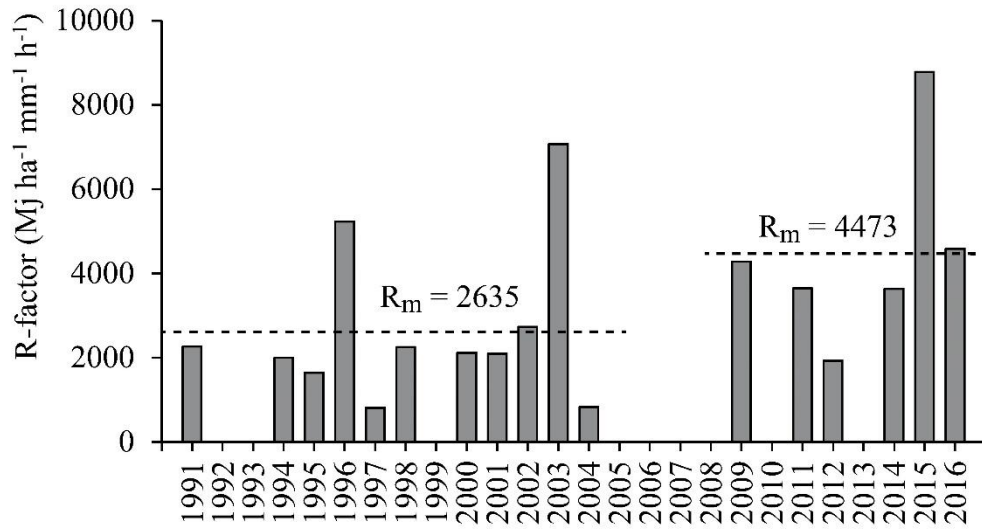
471

472 **Fig. 5** Spatial vision of the trees from each plot (A-D) and corresponding spatial distribution of soil erosion (E-H). Figure 5C shows a photo of the Plot 3 where cutting  
 473 operations were performed in 2009.

474



Gambarie meteo station



475

476 **Fig. 6** Rainfall erosivity factor for Gambarie meteo station

477